Environmental Science & Technology Letters

pubs.acs.org/journal/estlcu

Letter

Drinking Boiled Tap Water Reduces Human Intake of Nanoplastics and Microplastics

Zimin Yu, Jia-Jia Wang, Liang-Ying Liu, Zhanjun Li,* and Eddy Y. Zeng*

Cite This: https://doi.org/10.1021/acs.estlett.4c00081

Read Online

ACCESS | Metrics & More | Article Recommendations | Supporting Information

ABSTRACT: Tap water nano/microplastics (NMPs) escaping from centralized water treatment systems are of increasing global concern, because they pose potential health risk to humans via water consumption. Drinking boiled water, an ancient tradition in some Asian countries, is supposedly beneficial for human health, as boiling can remove some chemicals and most biological substances. However, it remains unclear whether boiling is effective in removing NMPs in tap water. Herein we present evidence that polystyrene, polyethylene, and polypropylene NMPs can coprecipitate with calcium carbonate ($CaCO_3$) incrustants in tap water upon boiling. Boiling hard water (>120 mg L^{-1} of $CaCO_3$) can remove at least 80% of polystyrene, polyethylene, and polypropylene NMPs size between 0.1 and 150 μm. Elevated temperatures promote $CaCO_3$ nucleation on NMPs, resulting in the encapsulation and aggregation of NMPs within $CaCO_3$ incrustants. This simple boiling-water strategy can "decontaminate" NMPs from household tap water and has the potential for harmlessly alleviating human intake of NMPs through water consumption.

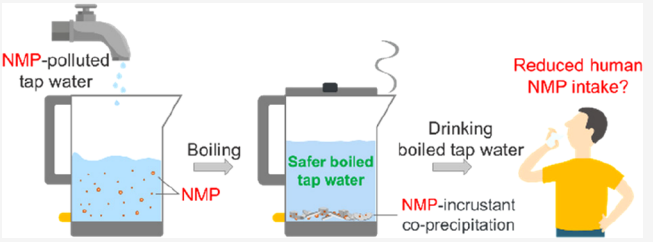

KEYWORDS: *Plastic particles, Tap water, Calcium carbonate, Coprecipitation, Human exposure*

INTRODUCTION

Nanoplastics (NPs, < 1 μm) and microplastics (MPs; 1−5000 μm)[1] are prevalent in global groundwater and surface water, which are the main sources of drinking water, and pose a threat to drinking water safety.[2,3] However, traditional centralized water treatment plants have limited capability to remove nano/microplastics (NMPs), especially NPs.[2,4] One hundred twenty-nine of 159 tap water samples from 14 countries worldwide contained NMPs, with polystyrene (PS), polyethylene (PE), polypropylene (PP), and polyethylene terephthalate (PET) as the most dominant polymer types.[5,6] Nano/microplastics may accumulate in human tissues and cause potential chronic effects, such as gut microbiota dysbiosis, insulin resistance, and liver metabolic disorder.[7,8] Although various advanced water treatment technologies were developed for removing NMPs,[9] only traditional processes were affordable in many developing and/or undeveloped areas.[10] Therefore, developing a simple and affordable household treatment process to remove NMPs from drinking water is significant for dealing with the global NMP threat.

Drinking boiled water is an ancient tradition in some Asian countries such as China, Vietnam, and Indonesia;[11,12] however, tap water (or filtered tap water) is often consumed directly in many western developed countries.[13] Boiling or heating tap water is able to remove trace pollutants such as disinfection byproducts[14,15] and some metal ions (e.g., Ca^{2+}, Cu^{2+}, and Mg^{2+}).[16,17] Boiling water with certain hardness and alkalinity commonly produces incrustants dominated by insoluble calcium carbonate ($CaCO_3$). Nano/microplastics could be encapsulated by newly generated $CaCO_3$, coprecipitating in aquatic ecosystems,[18] and could even promote $CaCO_3$ biomineralization.[19] Removal of NMPs from drinking water can be realized by coagulation and precipitation. However, it is unclear whether the formation of water incrustants during the boiling process can remove NMPs.

Herein we simulated the boiling process of tap water containing commercial fluorescent PS microspheres (1 and 0.1 μm), used as model NPs for their defined size, high fluorescence intensity, easily accessible surface chemistry (i.e., functionalization), and commercial availability,[20] to assess the impacts of water temperature, water hardness, and NP concentration and property on the coprecipitation of NPs and water incrustants. Additional experiments were conducted with MPs (100−150 μm), including commercial PS and environmental PE and PP aged under sunlight for 60 d, to verify the results with NPs to be also applicable to MPs. Combining NMP precipitation efficiencies with a series of water hardness values, we estimated the global human exposure to NMPs through drinking boiled water. This study

Received: January 29, 2024
Revised: February 6, 2024
Accepted: February 7, 2024

Table 1. Overview of the Experimental Conditions of Nano/Microplastics Including Polystyrene (PS) Sphere, Polyethylene (PE) Fragment, and Polypropylene (PP) Fiber During Boiling

Species	Size (μm)	Functional group	Concentration (mg L^{-1}/particle μL^{-1})	Water hardness (mg L^{-1})	Temperature (°C)
PS sphere	1	Bare	1/31 ± 2.0	180	25−100
	1	Bare	1/31 ± 2.0	0−300	100
	1/0.1	Bare	0−5/0−360	180	100
	1/0.1	Bare/carboxyl/amino	1/31−91	180	25−100
	100	Bare	1/0.0028 ± 0.000078	180	25−100
PE fragment	150	-	-/0.00075	180	25−100
PP fiber	100	-	-/0.00075	180	25−100

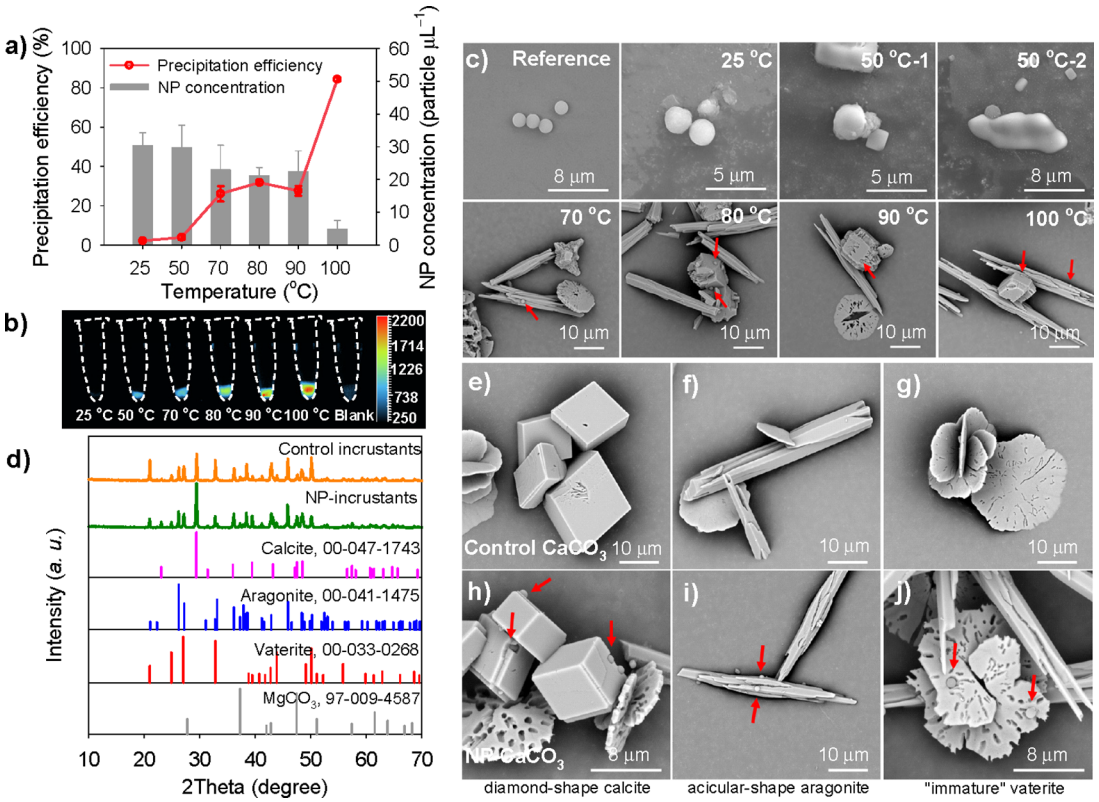

Figure 1. Bare-polystyrene nanoplastic (NP, 1 μm, 1 mg L^{-1}, 3.1 ± 2.0 particle μL^{-1}) and incrustant coprecipitates during boiling of tap water (180 mg L^{-1} of $CaCO_3$). (a) NP precipitation efficiencies in the supernatants at 25−100 °C; (b) Fluorescence imaging results of incrustants at 25−100 °C; (c) Scanning electron microscopic (SEM) images of reference NP (Reference) and incrustants began to grow on NP surface and finally encapsulated NP at 25−100 °C; (d) X-ray diffraction patterns of control incrustants without NP (Control incrustants) and coprecipitates of NP and incrustants (NP-incrustants) upon boiling (100 °C); (e−g) SEM images of control calcium carbonate crystals without NP (Control $CaCO_3$); and (h−j) coprecipitates of NP and calcium carbonate crystal (NP-$CaCO_3$) upon boiling (100 °C). Red arrows indicated NPs.

aimed to stimulate more studies, setting the foundation for establishing a healthy water consumption habit to reduce the risk of global human exposure to NMPs exposure.

METHODS AND MATERIALS

Preparation and Pretreatment of Water Samples. Detailed information regarding materials can be found in Text S1. Solutions of fluorescent PS, calcium chloride, and sodium bicarbonate, tap water collected from Guangzhou, China (180 mg L^{-1} of $CaCO_3$), and deionized water with resistivity of 18 MΩ-cm (QClean CCT-3300, Dongguan, China) were mixed and treated for different purposes.

Tap water samples mixed with 40 μL bare-PS (1 μm, 1000 mg L^{-1}), with final NP concentration at 1 mg L^{-1} (~31 ± 2.0 particles μL^{-1}), were separately heated at 25−90 °C and boiled at 100 °C.[21] Deionized water samples containing NPs (bare-PS, 1 μm, 1 mg L^{-1}) were adjusted with water hardness in a range of 0−300 mg L^{-1} of $CaCO_3$[22] and boiled. Tap water samples containing NPs with a series of NP concentrations (bare-PS, 1 and 0.1 μm, 0−5 mg L^{-1}, 0−360 particles μL^{-1}) were boiled at 100 °C. Tap water samples were separately mixed with six types of NPs including three surface function groups (bare-, carboxyl-, and amino-) with two particle sizes (1 and 0.1 μm), with final NP concentrations at 1 mg L^{-1}, and were separately treated at 25−100 °C. All experimental parameters and conversion ratios of number and mass concentrations of NPs are listed in Table 1 and Table S1, respectively.

For all PS NP water samples, the final volume of the mixed solutions was 40 mL. The mixed water solutions were agitated in an ultrasonic bath for 20 min to disperse particles evenly.[23] Heating/boiling continued for another 5 min after the preset temperature was reached on an electronic hot plate.[13] After heating/boiling, the mixed solutions were left to cool for 10

https://doi.org/10.1021/acs.estlett.4c00081
Environ. Sci. Technol. Lett. XXXX, XXX, XXX−XXX

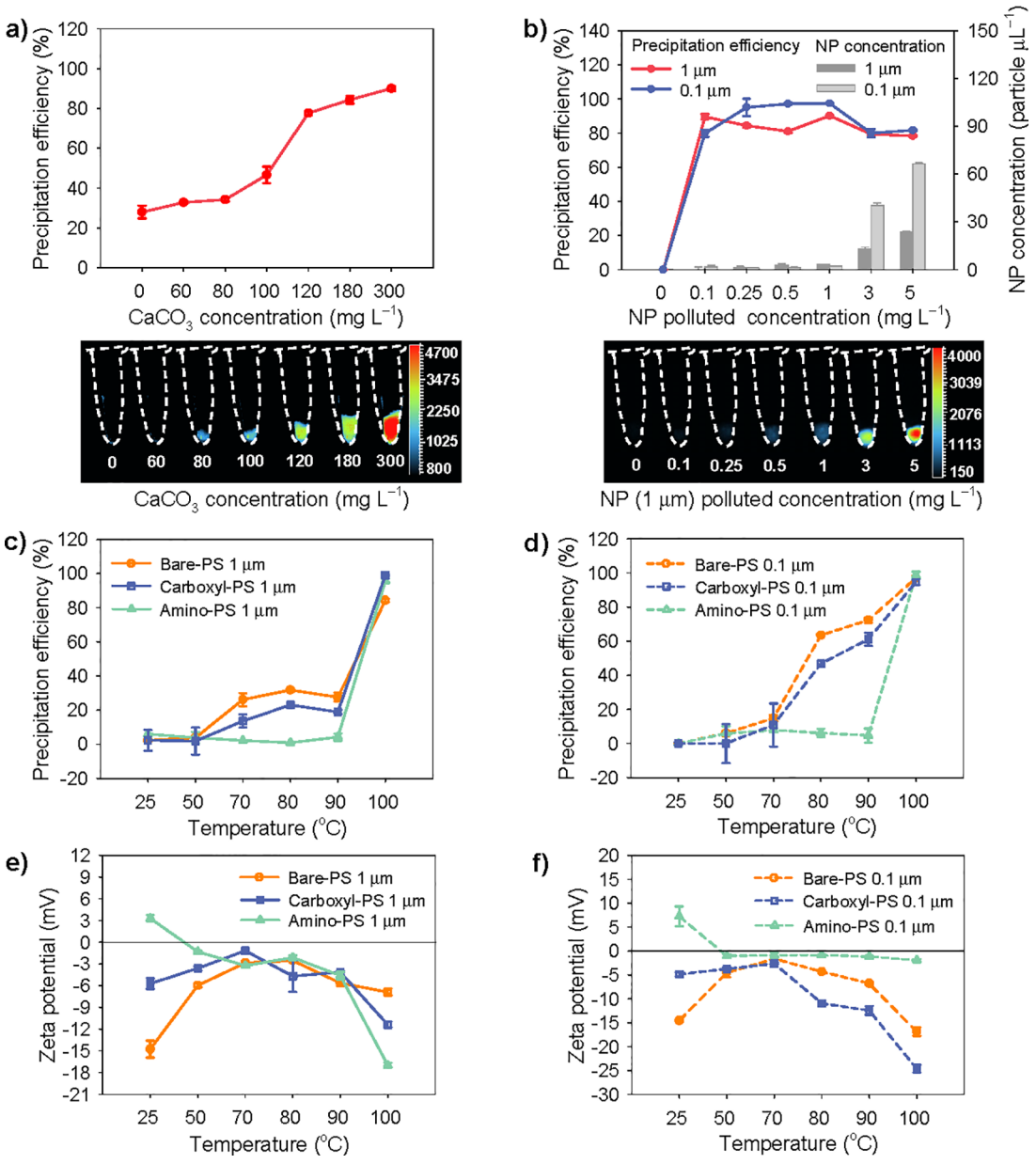

Figure 2. Influence factors on the formation of nanoplastic (NP) and incrustant coprecipitates at different temperatures. (a) Bare-polystyrene (PS, 1 μm, 1 mg L^{-1}, 3.1 ± 2.0 particle μL^{-1}) NP precipitation efficiency and fluorescence images of incrustants in different water hardness upon boiling (100 °C); (b) Bare-PS NP precipitation efficiency and fluorescence images of incrustants in different NP concentrations upon boiling of tap water (180 mg L^{-1} of $CaCO_3$, 100 °C); and (c,d) NP precipitation efficiency and (e,f) Zeta potential of 1 and 0.1 μm bare-, carboxyl-, and amino-PS in tap water (180 mg L^{-1} of $CaCO_3$) at 25−100 °C. Conversion ratios of number and mass concentrations of PS NPs are listed in Table S1.

min. Each experiment was repeated three times. A supernatant sample at 1 mL was collected from a 1 cm depth below the supernatant surface for flow cytometry analysis (Figure S1). Precipitates were separated for further characterization. Rigorous measures were implemented to minimize cross contamination (Text S2).

In addition to PS NPs, supernatant and precipitate samples for the separate boiling event with field commonly detected MPs including PS sphere (~100 μm), PE fragment (~150 μm), and PP fiber (~100 μm) were analyzed (Table 1, Text S3, and Figure S2).

Flow Cytometric Analysis of Supernatant Fluorescent Nanoplastics. Compared with commonly used techniques such as micro-Fourier transform infrared and Raman microspectroscopy, flow cytometry can provide absolute quantification of fluorescent NMPs, make multiple measurements, and reduce time and manpower.[24,25] A Northern Light 3000 flow cytometer (Cytek Biosciences; Fremont, CA) was used to determine supernatant NP concentrations (Text S4 and Figure S3). The NMP precipitation efficiency (η) was calculated by

$$\eta = (C_0 - C)/C_0 \quad (1)$$

where C_0 and C are the NMP concentrations before and after heating/boiling, respectively.

Identification and Characterization of Precipitates. A fluorescence imaging system (UVP Chemstudio touch, Analytik Jena, Germany) was employed to trace the migration of NPs in water during the boiling process.[26] A X-ray diffractometer (D2-Phaser, Bruker Instruments, Germany) was acquired to investigate the crystal lattice structure of NP

https://doi.org/10.1021/acs.estlett.4c00081
Environ. Sci. Technol. Lett. XXXX, XXX, XXX−XXX

and incrustant coprecipitates. A scanning electron microscope (S-4800, Hitachi, Tokyo, Japan) was used to observe the microstructures of the coprecipitates.

Assessment of Human Exposure to Nano/Microplastics through Drinking Water Consumption. The NMP concentration data in tap water from six continents, including Asia, Europe, North America, South America, Africa, and Oceania, were extracted from the literature (Table S2). The average intake of NMPs from boiled water (NMP_{boiled}) and tap water (NMP_{tap}) associated with daily consumption of boiled and tap water were assessed by

$$NMP_{boiled} = C_{NMP} \times \eta \times IR_{boiled} \quad (2)$$

$$NMP_{tap} = C_{NMP} \times IR_{tap} \quad (3)$$

where C_{NMP} is the average NMP concentrations in tap water from different sources (Table S2); η is the NMP precipitation efficiency (Table S3); and IR_{boiled} and IR_{tap} represent daily intake rate via boiled and tap water, respectively (Table S4).

RESULTS AND DISCUSSION

Coprecipitation of Nanoplastics with Water Incrustants during Boiling Process. Supernatant NP removal efficiency gradually increased initially from 2 ± 0.15% to 28 ± 2.6 during the heating process (25−90 °C), and sharply increased to 84 ± 1.1% at 100 °C (Figure 1a and Table S5). Concurrently the NP concentration decreased from 30 ± 4.0 to 4.8 ± 2.6 particle μL^{-1} (Figure 1a and Table S5), and disappeared supernatant NPs were transferred into incrustants (Figure 1b). Increasing the temperature accelerated the formation of incrustants (Figure S4a), resulting in an increased NP concentration in the precipitates. The highest NP concentration in the precipitates occurred at 100 °C when the incrustants were most abundant (Figure 1b and Table S6). Apparently boiling prevalently facilitated the removal of NPs from tap water due to coprecipitation of NPs and incrustants. Incrustants began to grow on the NP surface at 50 °C and encapsulate NPs at 70 °C (Figure 1c) when residual NPs in the supernatant started to decline, further confirming that the decrease of residual NPs in the supernatant was synchronized with the formation of incrustants.

Three different $CaCO_3$ polymorphs were observed in the incrustants with and without NPs (Figure 1d−j and Table S7), including diamond-shape calcite (JCPDS No. 00-047-1743), acicular-shape aragonite (JCPDS No. 00-041-1745), and disk-like and/or sunflower-like shape vaterite (JCPDS No. 00-033-0268) which was considered as "immature" vaterite.[16] Tiny magnesium carbonate crystals ($MgCO_3$; JCPDS No. 97-009-4587) were also detected, probably ascribed to the presence of trace-level magnesium ions in tap water (Figure 1d and Table S7). The morphology and polymorph structure of $CaCO_3$ crystals can be achieved by various synthesis techniques at controlled nonboiling temperatures.[27] However, controlling crystal growth during boiling is quite difficult as bubbling causes strong turbulence,[28] resulting in heterogeneous microenvironments for crystal growth and random occurrence of different $CaCO_3$ crystal phases.[29] Nanoplastics were either encapsulated in calcite, aragonite, and vaterite crystals or attached to the growing planes of $CaCO_3$ crystals (Figure 1h−j). The $CaCO_3$ crystals could embrace NPs effectively upon boiling, so the $CaCO_3$ polymorph may not be a predominant factor for NP precipitation.

Factors Affecting Precipitation of Nanoplastics during Boiling. Drinking water hardness varies significantly with different regions[17] and may influence the efficiency of removing NPs by boiling. Our results showed that NP precipitation efficiency increased with increasing water hardness upon boiling (Figure 2a), for example, from 34% at 80 mg L^{-1} to 84% and 90% at 180 and 300 mg L^{-1} of $CaCO_3$, respectively (Table S5). Even with soft water (<60 mg L^{-1} of $CaCO_3$),[22] boiling can still remove more than 25% of NPs. In addition to the coprecipitation of NP and incrustants (Figure S4b), high temperatures can increase the collision frequency and attachment of NPs which may aggregate and increase in size, resulting in gravitational settling.[30]

The concentration threshold for the effective removal of NPs upon boiling was assessed. The precipitation efficiencies of both 1 and 0.1 μm NPs were maintained at 80−97% upon boiling within the entire NP concentration range, and incrustants were combined with NPs more intensively at higher NP concentration (Figure S4c). However, the concentrations of residual supernatant NPs for both sizes showed an increasing trend upon boiling when they were >1 mg L^{-1} (Figure 2b). Certain amounts of $CaCO_3$ incrustants are produced after boiling if Ca^{2+} concentrations remain constant in tap water, and these $CaCO_3$ incrustants would combine with only a limited number of NPs. Once excessive NPs occur in tap water (e.g., in the case of 3 mg L^{-1}), $CaCO_3$ incrustants are unable to combine with all superabundant NPs, resulting in a high residual NP concentration in boiled water. It is worth noting that NP concentrations in global tap water are generally below 1 mg L^{-1} (~31 ± 2.0 particle μL^{-1}) (Table S2), thus boiling may be a feasible process to reduce the global population exposure to NPs.

Surface functional groups on NPs may influence NPs transport in tap water.[21] During the heating process (25−90 °C), the precipitation efficiencies of bare-PS and carboxyl-PS were mostly higher than those of amino-PS for both 1 and 0.1 μm sizes (Figure 2c,d). This may be attributed to the presence of negative surface charges (Figure 2e,f) on both bare-PS and carboxyl-PS, which attracts Ca^{2+} and accelerates nucleation and growth of $CaCO_3$ crystals.[18] On the contrary, positive surface charges on amino-PS at the initial stage (Figure 2e,f) would resist crystal nucleation and aggregation of PS particles. When the water temperature increased, the zeta potential of the positively charged amino-PS decreased, and the water system could overcome the energy barrier and generate charge reversal (Figure 2e,f). High temperature may enhance the interaction between amino-PS and $CaCO_3$ crystals,[31,32] which may be associated with the thermodynamic driving force of $CaCO_3$ crystal formation that can be expressed by supersaturation (S),[16,33] $S = \{[\alpha\ (Ca^{2+}) \times \alpha\ (CO_3^{2-})] \div K_{sp}\}^{1/2}$, where α represents ionic activity and K_{sp} designates the thermodynamic solubility product of $CaCO_3$ precipitates which decreases with increasing temperature.[16,33] During the heating process, S rose and $CaCO_3$ crystallization rate increased,[16] and the zeta potential decreased (Figure 2e,f) with lessening electrostatic repulsion interaction between particles,[34] so that the aggregation of NPs and $CaCO_3$ crystals was enhanced. At boiling point (100 °C), all surface functionalized NPs showed good precipitation efficiency; that is, they could well coprecipitate with $CaCO_3$ crystals.

Particle size is another factor controlling the precipitation efficiency of NPs. For bare-PS and carboxyl-PS, the precipitation efficiencies were higher for 0.1 μm NPs than

https://doi.org/10.1021/acs.estlett.4c00081
Environ. Sci. Technol. Lett. XXXX, XXX, XXX−XXX

for 1 μm ones when $CaCO_3$ crystals started to form (80−90 °C). Because 0.1 μm NPs have larger specific surface areas than 1 μm NPs, they are more likely to form nucleation sites and are quickly encapsulated by $CaCO_3$ crystals, thus preferentially settling during heating (Figure 2c,d). Amino-PS may resist crystal nucleation as it possesses a positive surface charge, so heating has little effect on the precipitation efficiency of amino-PS (Figure 2c,d). Different morphologies of crystals, which were the transition forms of vaterite, occurred in 1 and 0.1 μm NP-incrustant coprecipitates (Figure S4d,e). As vaterite is a more thermodynamically unstable polymorph than calcite and aragonite, its morphology easily transforms at high temperatures.[16] The interfaces of different-sized particles may have different contact angles which control the $CaCO_3$ nucleation rate and influence crystal growth,[35,36] and various morphologies of "immature" vaterite occurred. Nevertheless, most NPs could precipitate upon boiling, regardless of NP sizes and incrustant phases. The present study highlights the likelihood that a simple boiling process can greatly complement traditional water treatments in effectively removing NPs.

Mechanisms for Coprecipitation of Nano/Microplastics and $CaCO_3$ Incrustants. According to the classical crystal nucleation theory, crystallization begins with random collisions of solute monomers (i.e., ions) until the clusters reach critical size and nucleus form, triggering nucleus growth.[35,37] As $CaCO_3$ crystals grow on NP surfaces and finally encapsulate NPs (Figure 1c), there may be an interfacial nucleation-encapsulation mechanism that governs the coprecipitation of NPs and $CaCO_3$ crystals (Figure S5). Dissolved H_2CO_3 and HCO_3^- decompose at high temperatures and form CO_3^{2-}. Ca^{2+} reacts with CO_3^{2-} to form $CaCO_3$ nuclei at NP-water interface because of decreased nucleation potential barrier in the presence of impurities.[35] Nanoplastics become encapsulated in $CaCO_3$ polymorphs (i.e., calcite, aragonite, and vaterite) during crystal growth (Figure 1c). The zeta potential decreases as strong Brownian motion increases the particle collision frequency (Figure 2e,f), and most NPs are attracted to the growing $CaCO_3$ crystal planes leading to heteroaggregation between NPs and $CaCO_3$ crystals.[31,32] When the growth of $CaCO_3$ crystals is complete, attracted NPs are continuously encapsulated by newly generated $CaCO_3$ crystals (Figure 1c).[18] Some NPs may deposit into immature $CaCO_3$ crystals directly before full crystal growth is complete. Upon boiling, $CaCO_3$ incrustants are formed by the reaction of Ca^{2+} with CO_3^{2-}, and most NPs are combined with $CaCO_3$ and precipitate under gravity. The mechanism is further confirmed by the coprecipitation of PS, PE, and PP MPs and incrustants (Text S3 and Figure S2).

Reduced Human Nano/Microplastic Exposure by Drinking Boiled Water. From various global water qualities (Figure 3a) and water consumption habits, we estimated intakes of NMPs by adults and children through drinking boiled and tap water in 67 regions on six continents. Intakes of NMPs through boiled water consumption are 2−5 times less than those through tap water on a daily basis (Figure 3b). Drinking boiled water apparently is a viable long-term strategy for reducing global exposure to NMPs. Drinking boiled water, however, is often regarded as a local tradition and prevails only in a few regions.[38] A large proportion of the global population maintains the habit of drinking tap and/or bottled water, unintentionally overlooking the issue of NMPs exposure.[11,38]

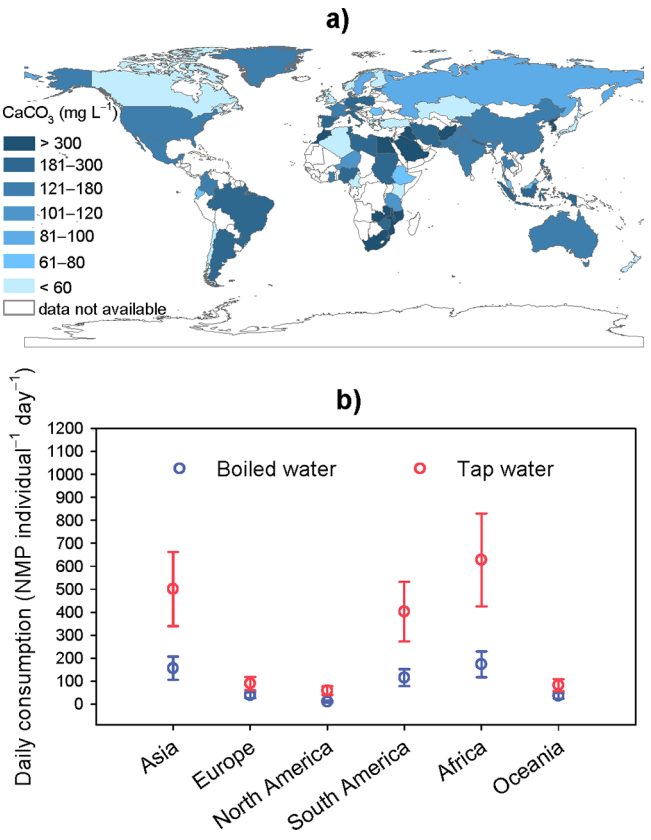

Figure 3. Daily human exposure to nano/microplastics (NMPs) through drinking water consumption. (a) World map of drinking water hardness (Table S3); (b) Daily consumption of NMPs through boiled and tap water in 67 regions of Asia, Europe, North America, South America, Africa, and Oceania, averaged across the adult and child, female, and male categories (both average and standard deviation values were determined).

Nonplastic electric kettles and gas stoves are recommended to prepare boiled water for their low energy consumption and low CO_2 emissions (Text S5, Tables S8−S10, and Figure S6). Taking China as an example, the energy consumption and CO_2 emissions related to boiling water accounted for ∼0.5% of the total energy consumption and ∼1% of the total CO_2 emissions, respectively. Filtration devices (e.g., stainless steel filters which are frequently used when drinking tea) are also recommended to retain NMP-incrustants when boiled water is consumed. Because the occurrence of NMPs and water quality are uneven globally, the efficacy of boiling water in reducing NMPs may vary from region to region. Nonetheless, our results have ratified a highly feasible strategy to reduce human NMP exposure and established the foundation for further investigations with a much larger number of samples.

■ ASSOCIATED CONTENT

Supporting Information

The Supporting Information is available free of charge at https://pubs.acs.org/doi/10.1021/acs.estlett.4c00081.

Detailed descriptions of the materials (Text S1); prevention of sample contamination and preparation of control samples (Text S2); sampling, methods, and results for MPs (Text S3); details of flow cytometric analysis for supernatant NP (Text S4); estimation of energy consumption and CO_2 emissions by boiling

https://doi.org/10.1021/acs.estlett.4c00081
Environ. Sci. Technol. Lett. XXXX, XXX, XXX−XXX

water (Text S5); conversion ratios of number and mass concentrations of NMPs (Table S1); occurrence of NMPs in global tap water (Table S2); global tap water hardness and the corresponding NMP precipitation efficiency (Table S3); recommended daily intake rate of water (Table S4); NP precipitation efficiency at different water temperature and hardness (Table S5); quantity of incrustants formed at different temperature (Table S6); X-ray diffraction standard cards of $CaCO_3$ and $MgCO_3$ (Table S7); energy consumption and CO_2 emissions by boiling 1 L water (Table S8); annual energy consumption and CO_2 emissions by boiling water (Table S9); global energy consumption and CO_2 emissions from energy consumption (Table S10); diagram of supernatant sampling location (Figure S1); coprecipitation of PS, PE, and PP MPs and incrustants (Figure S2); gating plots of flow cytometry (Figure S3); morphology and composition of incrustants in different conditions (Figure S4); diagram of the coprecipitated mechanism (Figure S5); proportions of energy consumption and CO_2 emissions related to boiling water (Figure S6) (PDF)

AUTHOR INFORMATION

Corresponding Authors

Zhanjun Li − *School of Biomedical Engineering, Guangzhou Medical University, Guangzhou 511436, China*; Email: zhanjunli@gzhmu.edu.cn

Eddy Y. Zeng − *Center for Environmental Microplastics Studies, Guangdong Key Laboratory of Environmental Pollution and Health, Jinan University, Guangzhou 511443, China*; orcid.org/0000-0002-0859-7572; Email: eddyzeng@jnu.edu.cn

Authors

Zimin Yu − *School of Biomedical Engineering, Guangzhou Medical University, Guangzhou 511436, China*

Jia-Jia Wang − *School of Biomedical Engineering, Guangzhou Medical University, Guangzhou 511436, China*; orcid.org/0000-0002-5176-6183

Liang-Ying Liu − *Center for Environmental Microplastics Studies, Guangdong Key Laboratory of Environmental Pollution and Health, Jinan University, Guangzhou 511443, China*; orcid.org/0000-0001-7867-1339

Complete contact information is available at: https://pubs.acs.org/10.1021/acs.estlett.4c00081

Notes

The authors declare no competing financial interest.

ACKNOWLEDGMENTS

The work was financially supported by the National Natural Science Foundation of China (Nos. 52172277 and 21936004). Special thanks go to Guangzhou Raybio Medical Technology for assistance in instrumental analysis.

REFERENCES

(1) Thompson, R. C.; Olsen, Y.; Mitchell, R. P.; Davis, A.; Rowland, S. J.; John, A. W. G.; McGonigle, D.; Russell, A. E. Lost at sea: Where is all the plastic? *Science* **2004**, *304*, 838−838.

(2) Li, Y.; Wang, Z.; Guan, B. Separation and identification of nanoplastics in tap water. *Environ. Res.* **2022**, *204*, 112134.

(3) Koelmans, A. A.; Mohamed Nor, N. H.; Hermsen, E.; Kooi, M.; Mintenig, S. M.; De France, J. Microplastics in freshwaters and drinking water: Critical review and assessment of data quality. *Water Res.* **2019**, *155*, 410−422.

(4) Pivokonsky, M.; Cermakova, L.; Novotna, K.; Peer, P.; Cajthaml, T.; Janda, V. Occurrence of microplastics in raw and treated drinking water. *Sci. Total Environ.* **2018**, *643*, 1644−1651.

(5) Tong, H.; Jiang, Q.; Hu, X.; Zhong, X. Occurrence and identification of microplastics in tap water from China. *Chemosphere* **2020**, *252*, 126493.

(6) Zhang, Y.; Diehl, A.; Lewandowski, A.; Gopalakrishnan, K.; Baker, T. Removal efficiency of micro- and nanoplastics (180 nm-125 um) during drinking water treatment. *Sci. Total Environ.* **2020**, *720*, 137383.

(7) Gao, B.; Shi, X.; Li, S.; Xu, W.; Gao, N.; Shan, J.; Shen, W. Size-dependent effects of polystyrene microplastics on gut metagenome and antibiotic resistance in C57BL/6 mice. *Ecotoxicol. Environ. Saf.* **2023**, *254*, 114737.

(8) Shi, C.; Han, X.; Guo, W.; Wu, Q.; Yang, X.; Wang, Y.; Tang, G.; Wang, S.; Wang, Z.; Liu, Y.; Li, M.; Lv, M.; Guo, Y.; Li, Z.; Li, J.; Shi, J.; Qu, G.; Jiang, G. Disturbed Gut-Liver axis indicating oral exposure to polystyrene microplastic potentially increases the risk of insulin resistance. *Environ. Int.* **2022**, *164*, 107273.

(9) Acarer, S. A review of microplastic removal from water and wastewater by membrane technologies. *Water Sci. Technol.* **2023**, *88* (1), 199−219.

(10) Zhu, Y.; Jiao, X.; Meng, W.; Yu, X.; Cheng, H.; Shen, G.; Wang, X.; Tao, S. Drinking water in rural China: Water sources, treatment, and boiling energy. *Environ. Sci. Technol.* **2023**, *57* (16), 6465−6473.

(11) Cohen, A.; Pillarisetti, A.; Luo, Q.; Zhang, Q.; Li, H.; Zhong, G.; Zhu, G.; Colford, J. M., Jr; Smith, K. R.; Ray, I.; Tao, Y. Boiled or bottled: Regional and seasonal exposures to drinking water contamination and household air pollution in rural China. *Environ. Health Perspect.* **2020**, *128*, 127002.

(12) Cohen, A.; Colford, J. M. Jr., Effects of boiling drinking water on diarrhea and pathogen-specific infections inlow- and middle-income countries: A systematic review and meta-analysis. *Am. J. Trop. Med. Hyg.* **2017**, *97*, 1362−1377.

(13) Pan, Y.; Zhang, X.; Wagner, E. D.; Osiol, J.; Plewa, M. J. Boiling of simulated tap water: Effect on polar brominated disinfection byproducts, halogen speciation, and cytotoxicity. *Environ. Sci. Technol.* **2014**, *48*, 149−156.

(14) Levesque, S.; Rodriguez, M. J.; Serodes, J.; Beaulieu, C.; Proulx, F. Effects of indoor drinking water handling on trihalomethanes and haloacetic acids. *Water Res.* **2006**, *40*, 2921−2930.

(15) Zhang, X. L.; Yang, H. W.; Wang, X. M.; Karanfil, T.; Xie, Y. F. Trihalomethane hydrolysis in drinking water at elevated temperatures. *Water Res.* **2015**, *78*, 18−27.

(16) Wu, Z.; Davidson, J. H.; Francis, L. F. Effect of water chemistry on calcium carbonate deposition on metal and polymer surfaces. *J. Colloid Interface Sci.* **2010**, *343*, 176−187.

(17) Shi, Y.; Li, D.; Xiao, L.; Sheerin, E. D.; Mullarkey, D.; Yang, L.; Bai, X.; Shvets, I. V.; Boland, J. J.; Wang, J. J. The influence of drinking water constituents on the level of microplastic release from plastic kettles. *J. Hazard. Mater.* **2022**, *425*, 127997.

(18) MatijakovićMlinarić, N.; Selmani, A.; Brkić, A. L.; NjegićDžakula, B.; Kralj, D.; Kontrec, J. Exposure of microplastics to organic matter in waters enhances microplastic encapsulation into calcium carbonate. *Environ. Chem. Lett.* **2022**, *20*, 2235−2242.

(19) Mahadevan, G.; Ruifan, Q.; Hian Jane, Y. H.; Valiyaveettil, S. Effect of polymer nano- and microparticles on calcium carbonate crystallization. *ACS Omega* **2021**, *6*, 20522−20529.

(20) Xu, E. G.; Cheong, R. S.; Liu, L.; Hernandez, L. M.; Azimzada, A.; Bayen, S.; Tufenkji, N. Primary and secondary plastic particles exhibit limited acute toxicity but chronic effects on Daphnia magna. *Environ. Sci. Technol.* **2020**, *54*, 6859−6868.

(21) World Health Organization. Microplastics in drinking water. 2019. See the following: https://www.who.int/publications/i/item/9789241516198

(22) World Health Organization. Hardness in drinking-water: Background document for development of WHO *Guidelines for Drinking-Water Quality*. 2010. See the following: https://iris.who.int/bitstream/handle/10665/70168/WHO_HSE_WSH_10.01_10_Rev1_eng.pdf
(23) Zhou, C.; Lu, C.; Mai, L.; Bao, L.; Liu, L.; Zeng, E. Y. Response of rice (Oryza sativa L.) roots to nanoplastic treatment at seedling stage. *J. Hazard. Mater.* **2021**, *401*, 123412.
(24) Hyeon, Y.; Kim, S.; Ok, E.; Park, C. A fluid imaging flow cytometry for rapid characterization and realistic evaluation of microplastic fiber transport in ceramic membranes for laundry wastewater treatment. *Chem. Eng. J.* **2023**, *454*, 140028.
(25) Tse, Y. T.; Lo, H. S.; Chan, S. M. N.; Sze, E. T. P. Flow cytometry as a rapid alternative to quantify small microplastics in environmental water samples. *Water* **2022**, *14*, 1436.
(26) Xia, Y.; Xiang, X. M.; Dong, K. Y.; Gong, Y. Y.; Li, Z. J. Surfactant stealth effect of microplastics in traditional coagulation process observed via 3-D fluorescence imaging. *Sci. Total Environ.* **2020**, *729*, 138783.
(27) Febrida, R.; Setianto, S.; Herda, E.; Cahyanto, A.; Joni, I. M. Structure and phase analysis of calcium carbonate powder prepared by a simple solution method. *Heliyon* **2021**, *7*, No. e08344.
(28) Varnaseri, M.; Peyghambarzadeh, S. M. Particulate fouling during boiling heat transfer and crystallization of CaCO3 aqueous solutions. *Heat and Mass Transfer* **2023**, *59*, 1477−1505.
(29) Pritula, I.; Sangwal, K. 29 - Fundamentals of crystal growth from solutions. *Handbook of Crystal Growth (Second Edition)* **2015**, 1185−1227.
(30) Singh, N.; Tiwari, E.; Khandelwal, N.; Darbha, G. K. Understanding the stability of nanoplastics in aqueous environments: Effect of ionic strength, temperature, dissolved organic matter, clay, and heavy metals. *Environ. Sci. Nano* **2019**, *6*, 2968−2976.
(31) Yu, S.; Li, Q.; Shan, W.; Hao, Z.; Li, P.; Liu, J. Heteroaggregation of different surface-modified polystyrene nanoparticles with model natural colloids. *Sci. Total Environ.* **2021**, *784*, 147190.
(32) Pradel, A.; Catrouillet, C.; Gigault, J. The environmental fate of nanoplastics: What we know and what we need to know about aggregation. *NanoImpact* **2023**, *29*, 100453.
(33) Ma, M.; Wang, Y.; Cao, X.; Lu, W.; Guo, Y. Temperature and supersaturation as key parameters controlling the spontaneous precipitation of calcium carbonate with distinct physicochemical properties from pure aqueous solutions. *Cryst. Growth Des.* **2019**, *19*, 6972−6988.
(34) Muhib, M. I.; Uddin, M. K.; Rahman, M. M.; Malafaia, G. Occurrence of microplastics in tap and bottled water, and food packaging: A narrative review on current knowledge. *Sci. Total Environ.* **2023**, *865*, 161274.
(35) Wu, K.; Tse, E. C. M.; Shang, C.; Guo, Z. Nucleation and growth in solution synthesis of nanostructures - From fundamentals to advanced applications. *Prog. Mater. Sci.* **2022**, *123*, 100821.
(36) Wang, C.; Wei, W.; Zhang, Y.-T.; Dai, X.; Ni, B.-J. Different sizes of polystyrene microplastics induced distinct microbial responses of anaerobic granular sludge. *Water Res.* **2022**, *220*, 118607.
(37) Teng, H. H. How ions and molecules organize to form crystals. *Elements* **2013**, *9*, 189−194.
(38) Cohen, A.; Zhang, Q.; Luo, Q.; Tao, Y.; Colford, J. M., Jr; Ray, I. Predictors of drinking water boiling and bottled water consumption in rural China: A hierarchical modeling approach. *Environ. Sci. Technol.* **2017**, *51*, 6945−6956.

https://doi.org/10.1021/acs.estlett.4c00081
Environ. Sci. Technol. Lett. XXXX, XXX, XXX−XXX